Preparation, characterization and in vitro antioxidant and anticancer studies of some 2,4-dichloro-*N*-[di(alkyl/aryl)carbamothioyl]benzamide derivatives

N. Gunasekaran,[a,*] V. Vadivel,[b] and Nathan R. Halcovitch, Edward R. T. Tiekink

[a] *Centre for Nanotechnology & Advanced Biomaterials (CeNTAB), SASTRA University, Thanjavur 613 401, India*

[b] *Center for Advanced Research in Indian System of Medicine (CARISM), SASTRA University, Thanjavur 613 401, India*

[c] *Department of Chemistry, Lancaster University, Lancaster LA1 4YB, United Kingdom*

[d] *Research Centre for Crystalline Materials, Faculty of Science and Technology, Sunway University, 47500 Bandar Sunway, Selangor Darul Ehsan, Malaysia*

ABSTRACT

In the present study, three biologically active, substituted acyl thiourea compounds (**1**–**3**) have been synthesized from 2,4-dichlorobenzoyl chloride, potassium thiocyanate and the corresponding secondary amine in dry acetone. The synthesized compounds were characterized by elemental analyses, UV–Visible, FT-IR, ^{1}H & ^{13}C NMR spectroscopic techniques. The molecular structures of **1**–**3** were determined by single crystal X-ray crystallography which shows twists of up to 70º about the (S=)**C–N**C(=O) bonds. All the synthesized compounds show good antioxidant and anticancer potential, in particular, compound **2** derived from di-n-propylamine.

Keywords: Thiourea derivatives, X-ray crystallography, Antioxidant activity, Cytotoxicity, EAC cell line

---

* Corresponding author. Tel.: +914362304346; fax: +91 4362 264120.

E-mail address: sciguna@scbt.sastra.edu (N. Gunasekaran).

Introduction

The significance of acylthiourea derivatives has been investigated for over a century and their results have proven diverse applications of acylthioureas in various fields. Thiourea derivatives have widely been used in analytical and process chemistry applications [1]. For the liquid–liquid extraction and pre-concentration of platinum group metals, *N*,*N*-dialkyl-*N´*-acylthioureas were used as ionophores [2]. Transition-metal complexes comprising *N*,*N*-dialkyl-*N´*-acylthioureas ligands acted as effective catalysts in oxidation catalysis [3-6]. Many corrosion studies confirmed the corrosion prevention ability of acylthioureas on the surface of a wide range of metals in different corrosive environments [7–9]. Acylthioureas are convenient synthons for the preparation of versatile heterocyclic compounds through cyclization [10,11]. Particularly relevant to the present investigation is that thiourea derivatives are well known for their biological activities such =as antimicrobial [12,13], antifungal [14], antibacterial [15], insecticidal [16], herbicidalactivity [17], etc. Polysubstituted acylthiourea and its fused heterocycle derivatives were utilized as inhibitors of influenza virus [18]. In addition, acylthiourea derivatives and their coordination compounds exhibit strong antitumor and anticancer activity [19]. Benzoylphenylthiourea derivatives possess potent antitumor activity

against both pancreatic and prostate cancer cell lines [20]. Thiourea derivatives bearing benzothiazole moiety have been used as powerful anticancer agents [21]. We report herein the synthesis and X-ray crystallographic studies of three new derivatives, namely 2,4-dichloro-*N*-(diphenylcarbamothioyl)benzamide (**1**), 2,4-dichloro-*N*-(dipropylcarbamothioyl)benzamide (**2**) and 2,4-dichloro-*N*-(dibutylcarbamothioyl)benzamide (**3**) and their in vitro antioxidant and anticancer studies.

Experimental

Materials and methods

All chemicals used in this work were procured from commercial sources and utilized without further purification. The organic solvents were distilled and purified according to literature procedures. Elemental analyses were performed by a Vario EL AMX-400 elemental analyzer. Uncorrected melting points were obtained in open capillary tubes on a Sigma melting point apparatus. FT-IR spectra in the mid-IR region (4000–600 cm^{-1}) were recorded on a Nicolet iS5 FT-IR spectrophotometer with KBr pellets. UV-vis spectra in the range 800 to 200 nm were recorded in ethanol solutions using a PG Instruments double-beam UV-vis spectrophotometer (Model T90+) with a quartz cell of 1 cm path length. ^{1}H and ^{13}C NMR spectra were recorded on BrukerAvance 400 MHz instrument in DMSO-d_6 with TMS as an internal standard.

Synthesis

A solution of 2,4-dichlorobenzoyl chloride (1.0473 g, 5 mmol) in acetone (50 mL) was added drop wise to a suspension of potassium thiocyanate (0.4859 g, 5 mmol) in anhydrous acetone (50 mL). The reaction mixture was heated under reflux for 45 minutes and then cooled

to room temperature. A solution of diphenyl amine / di-n-propyl amine / di-n-butyl amine (0.5059–0.8461 g, 10 mmol) in acetone (30 mL) was added and the resulting mixture was stirred for 2 h at room temperature. Hydrochloric acid (0.1 N, 500 mL) was added and the resulting white solid was filtered off, washed with water and dried in vacuo. Single crystals of **1**-**3** for X-ray diffraction studies were grown at room temperature from their respective dichloromethane solutions.

*Synthesis of 2,4-dichloro-N-(diphenylcarbamothioyl)benzamide **(1)***

Yield: 90%. Orange solid. m.p. 162 ^{o}C. Anal. Calc. for $C_{20}H_{14}Cl_2N_2OS$ (%): C, 59.86; H, 3.52; N, 6.98; S, 7.99. Found: C, 59.80; H, 3.51; N, 6.94; S, 7.94. UV [Ethanol, λ in nm (ε in $dm^3mol^{-1}cm^{-1}$)]: 220 (98,247), 317 (37,216). FT–IR (KBr): ν = 3162 (N–H), 1691 (C=O), 1261 (C=S) cm^{-1}. ^{1}H NMR (DMSO-d_6): δ 11.42 (s, 1H, N–H), 7.02–7.74 (m, 13H, aromatic) ppm. ^{13}C NMR (DMSO-d_6): δ 183.2 (C=S), 161.7 (C=O), 117.1, 120.1, 127.4, 127.5, 127.7, 129.6, 129.7, 130.7, 131.5, 132.1, 133.6, 134.4, 136.0, 136.1, 145.8 (aromatic) ppm.

*Synthesis of 2,4-dichloro-N-(dipropylcarbamothioyl)benzamide (**2**)*

Yield: 85%. White solid. m.p. 153 ^{o}C. Anal. Calc. for $C_{14}H_{18}Cl_2N_2OS$ (%): C, 50.45; H, 5.44; N, 8.41; S, 9.62. Found: C, 50.41; H, 5.42; N, 8.37; S, 9.58. UV [Ethanol, λ in nm (ε in $dm^3mol^{-1}cm^{-1}$)]: 207 (30,240), 286 (8,522). FT–IR (KBr): ν = 3230 (N–H), 1661 (C=O), 1210 (C=S) cm^{-1}. ^{1}H NMR (DMSO-d_6): δ 10.90 (s, 1H, N–H), 7.46–7.69 (m, 3H, aromatic), 3.85 (t, 2H, CH_2), 3.54 (t, 2H, CH_2), 1.65–1.75 (m, 4H, CH_2), 0.85 (t, 3H, CH_3), 0.92 (t, 3H, CH_3) ppm. ^{13}C NMR (DMSO-d_6): δ 179.8 (C=S), 163.2 (C=O), 127.8, 129.7, 130.7, 131.8, 134.8, 135.6 (aromatic), 54.2, 54.6 (CH_2), 19.5, 21.7 (CH_2), 11.4, 11.5 (CH_3) ppm.

*Synthesis of 2,4-dichloro-N-(dibutylcarbamothioyl)benzamide (**3**)*

Yield: 88%. White solid. m.p. 157 ^{o}C. Anal. Calc. for $C_{16}H_{22}Cl_2N_2OS$ (%): C, 53.18; H, 6.14; N, 7.75; S, 8.87. Found: C, 53.11; H, 6.11; N, 7.70; S, 8.81. UV [Ethanol, λ in nm (ε in $dm^3mol^{-1}cm^{-1}$)]: 206 (15,085), 287 (4,432). FT–IR (KBr): ν = 3186 (N–H), 1678 (C=O), 1238 (C=S) cm^{-1}. ^{1}H NMR (DMSO-d_6): δ 10.87 (s, 1H, N–H), 7.46–7.71 (m, 3H, aromatic), 3.88 (t, 2H, CH_2), 3.56 (t, 2H, CH_2), 1.58–1.71 (m, 4H, CH_2), 1.58–1.71 (m, 4H, CH_2), 0.86–0.93 (m, 6H, CH_3) ppm. ^{13}C NMR (DMSO-d_6): δ 179.7 (C=S), 163.1 (C=O), 127.8, 129.7, 130.7, 131.8, 134.7, 135.7 (aromatic), 52.8, 52.4 (CH_2), 30.3, 28.2 (CH_2), 20.0, 19.9 (CH_2), 14.2, 14.0 (CH_3) ppm.

X-ray crystallography

Intensity data for **1**–**3** were measured at 100 K on a Agilent Technologies SuperNova Dual CCD with an Atlas detector using CuKα radiation, λ = 1.54184 Å [22]. The structures were solved by direct methods (SHELXS97 [23] through the WinGX Interface [24]) and refined (anisotropic displacement parameters, C-bound H atoms in the riding model approximation and a weighting scheme of the form $w = 1/[\sigma^2(F_o^2) + aP^2 + bP]$ where $P = (F_o^2 + 2F_c^2)/3$) with SHELXL2014/7 on F^2 [25]. The N-bound hydrogen atoms were located from difference maps and refined with N–H = 0.88±0.01 Å. In the refinement of **1**, the chloride atom at the C4 position of molecule 'a' was disordered over the C4/C8 positions. The major component had a site occupancy factor = 0.850(3). The analyzed sample was a two-component twin [twin law: -1 0 0, 0 -1 0, 0.721 0 1] and the minor component fraction was 0.3905(6). In the final refinement, 14 reflections with poor agreement were omitted. In the refinement of **3**, both molecules exhibited disorder in the

C4-bound chloride atoms. The major components had site occupancy factors = 0.8667(17) and 0.9379(18) for molecules 'a' and 'b', respectively. One of the n-butyl groups was also found to be disordered so that the C14 and C15 atoms were located over two positions; major component = 0.740(6). The molecular structure diagrams shown in Fig. 1 were drawn with 70% displacement ellipsoids [24], and overlay diagrams, also in Fig. 1, were drawn in QMol [26]. Crystallographic data are collated in Table 1. The crystal packing diagrams were generated with DIAMOND [27] with additional crystallographic analysis employing PLATON [28].

Table 1

Summary of the crystallographic data for **1**–**3**.

	1	**2**	**3**
Formula	$C_{20}H_{14}Cl_2N_2OS$	$C_{14}H_{18}Cl_2N_2OS$	$C_{16}H_{22}Cl_2N_2OS$
Formula weight	401.29	333.26	361.31
Crystal size (mm)	0.08 x 0.14 x 0.16	0.08 x 0.18 x 0.28	0.05 x 0.15 x 0.18
Crystal system	monoclinic	monoclinic	monoclinic
Space group	$P2_1/c$	$P2_1/c$	$P2_1/n$
a/Å	13.2182(2)	13.33360(10)	18.1370(4)
b/Å	14.3820(4)	23.7506(2)	9.66110(10)
c/Å	39.3125(6)	9.90310(10)	21.3995(3)
α/°	90	90	90
β/°	96.965(2)	91.0180(10)	106.520(2)
γ/°	90	90	90

V/Å^3	7418.3(3)	3135.63(5)	3594.91(11)
Z/Z'	16/4	8/2	8/2
D_c/g cm^{-3}	1.437	1.412	1.335
μ/mm^{-1}	4.294	4.942	4.351
θ range/°	3.3–77.5	3.3–77.3	2.8–77.6
Reflections measured	69016	26241	38181
Independent reflections; R_{int}	21284, 0.050	6594, 0.027	7576, 0.036
Reflections with $I > 2\sigma(I)$	19129	6286	6646
Number of parameters	960	371	447
R, obs. data; all data	0.041, 0.046	0.027, 0.028	0.038, 0.044
a; b in wght scheme	0.051; 7.608	0.040; 1.692	0.053; 2.356
R_w, obs. data; all data	0.108, 0.110	0.070, 0.071	0.097, 0.102
GoF (F^2)	1.05	0.95	1.04
$\Delta\rho_{max, min}$ (e Å^{-3})	0.79, -0.64	0.36, -0.38	0.54, -0.30

Antioxidant activity

Phosphomolybdate assay

The antioxidant activity of **1**–**3** was evaluated according to the method of Prieto *et al*. [29]. An aliquot of 100 µl of compounds was combined with 1 ml of reagent solution (0.6 M sulphuric acid, 28 mM sodium phosphate, and 4 mM ammonium molybdate) in a screw-capped vial. The vials were closed and incubated in a water bath at 95 °C for 90 min. After the samples

had cooled to room temperature, the absorbance of the mixture was measured at 695 nm against a blank. The results expressed as ascorbic acid equivalent antioxidant activity.

Ferric reducing power

The reducing power of the synthesized acythiourea derivatives was determined according to the method of Oyaizu [30]. Samples (2.5 ml) in phosphate buffer (2.5 ml, 0.2 M, pH 6.6) were added to potassium ferricyanide (2.5 ml, 1.0%) and the mixture was incubated at 50 °C for 20 min. Trichloroacetic acid (2.5 ml, 10%) was added, and the mixture was centrifuged at 650 x g for 10 min. The supernatant (5.0 ml) was mixed with ferric chloride (5.0 ml, 0.1%), and then the absorbance was read spectrophotometrically at 700 nm. Based on the absorbency value, the ferric reducing power of compounds was expressed.

DPPH radical scavenging activity

The DPPH radical scavenging activity was analyzed for each compound by following method of Sanchez-Moreno *et al*. [31]. The compounds (100 µl) was added to 3.9 ml of DPPH solution (0.025 g/L) and the reactants were incubated at 25 °C for 30 min. Different concentrations of ferulic acid was used as a positive control and ethanol was used instead of compounds in the blank (control). The decrease in absorbance was measured at 515 nm using a spectrophotometer. The radical scavenging activity of tested samples was calculated and expressed on percentage basis.

Superoxide radical scavenging activity

The capacity of prepared compounds to scavenge the superoxide anion radical was measured according to the method described by Zhishen *et al*. [32]. The reaction mixture was prepared using 3 x 10^{-6} M riboflavin, 1 x 10^{-2} M methionine, 1 x 10^{-4} M nitroblue tetrozolium chloride and 0.1 mM EDTA in phosphate buffered saline (pH 7.4). For the analysis, 3.0 ml of the reaction mixture was taken with 100 µl of compounds in closed tubes and illuminated for 40 min under fluorescent lamp (18 W). The absorbance was then read at 560 nm against the un-illuminated reaction mixture. Results were expressed as superoxide radical scavenging activity on a percentage basis.

Cytotoxicity

The anticancer potentialy of acylthiourea compounds was evaluated in the EAC cell line. The EAC cells were obtained from Swiss mice after 15 days of cancer induction. The peritoneal fluid containing EAC cells was collected aseptically using a 5 ml syringe and cultured in Dulbecco's modified Eagle's medium supplemented with 10% heat-inactivated foetal bovine serum, 1% nonessential amino acids, and 1% penicillin (5000 IU/mL)-streptomycin (5000 μL/mL) solution at 37 °C under 5% CO_2 atmosphere. Initially the cells were washed with PBS twice, centrifuged and the cell pellet was collected and re-suspended in DMEM medium and incubated at 37 °C for 2 days in a CO_2 incubator.

The anticancer effects of **1**–**3** was analyzed by treating with EAC cells for 24 h and the cell viability will be checked using MTT assay [33]. After attaining 60% confluency, the cells were trypsinized and dispersed in 96 well plate with a cell count of 9000 cells per well and incubated for 24 h. Then the compounds were added at different concentration and then again incubated for 24 h. At the end, the medium was discarded, cells are washed with PBS and 20

micro liter of MTT reagent was added in each well and incubated for 6 h at 37 ºC in a water bath. Then 150 micro liter of acidic isopropanol was added and shaken for 30 min on a plate shaker under dark. The absorbance was measured at 540 nm and the percentage of cell viability was calculated and from that the cytotoxic was derived.

Results and discussion

Synthesis

Compounds **1**–**3** were synthesized from 2,4-dichlorobenzoyl chloride, potassium thiocyanate and the corresponding secondary amine in dry acetone (Scheme 1). The compound **1** is orange while remaining compounds **(2** and **3)** are white. The synthesized compounds are air-stable and non-hygroscopic in nature, soluble in organic solvents such as *n*-hexane, ethyl acetate, acetone, acetonitrile, benzene, dichloromethane, chloroform, DMSO and DMF, and insoluble in water. The analytical data obtained are in good agreement with the proposed molecular formulae.

Spectroscopy

The synthesized acylthiourea compounds showed two bands around 206–220 and 286–317 nm in their UV-vis spectra, which are ascribed to π–π* and n–π* transitions, respectively. The FT–IR spectra of all the compounds exhibited very strong absorption bands around 3162–3230 cm^{-1} which suggest the presence of N–H group in their structures. The observation of a strong band in the region 1661–1691 cm^{-1} and a medium intensity band in the region 1210–1261 cm^{-1} in the FT–IR spectra of **1**–**3** confirmed the presence of

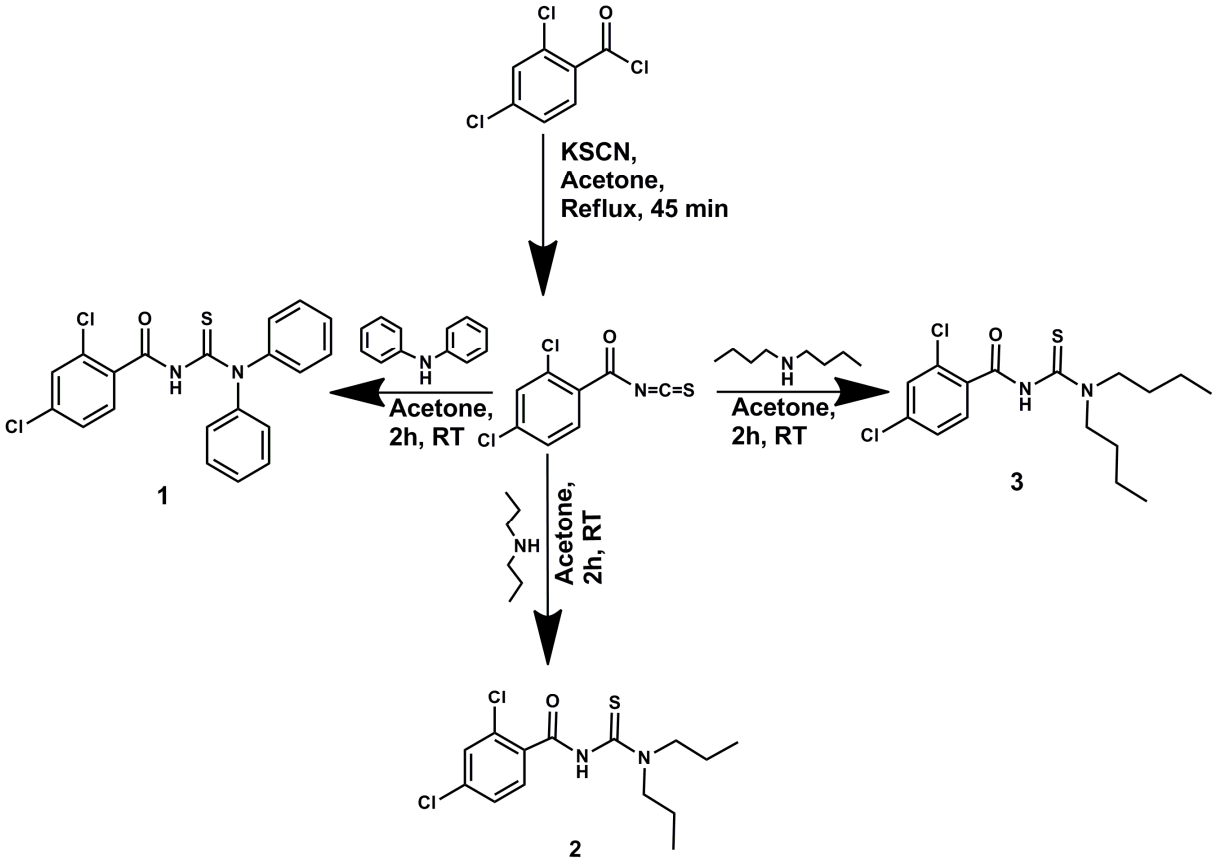

Scheme 1. Synthesis of acyl thiourea compounds.

C=O and C=S groups, respectively [5]. The ^{1}H NMR spectra showed a singlet around 10.87–11.42 ppm, which has been attributed to the N–H proton of ligands. The multiplets observed in the region 7.02–7.74 ppm, in the ^{1}H NMR spectra of all the compounds, have been assigned to the aromatic protons of the phenyl ring(s) present in the compounds. In addition, ^{1}H NMR spectrum of **2** showed two triplets at 3.85 and 3.54 ppm and a multiplet at 1.65–1.75 ppm, which were assigned to the methylene protons, and two triplets around 0.85 and 0.92 ppm which have been attributed to the terminal methyl protons. The duplication of the resonances are consistent with the non-equivalence of the n-propyl groups in solution; similar duplicity was noted for **3**. Thus, two triplets appeared at 3.56 and 3.88 ppm in the ^{1}H NMR spectrum of **3** due

to the protons of methylene groups which are proximate to nitrogen. ^{1}H NMR spectrum of **3** also exhibited two multiplets in the region 1.23–1.37 and 1.58–1.71 ppm, which were attributed to the remaining methylene protons of the aliphatic chain. A multiplet (merging of two triplets) at 0.86–0.93 ppm was assigned to the methyl protons. In the ^{13}C NMR spectra of **1**–**3** the signals observed around 128.3–146.4 ppm were assigned to the aryl carbons and signals appeared in the regions at 179.7–183.2 and 161.7–163.2 ppm have been ascribed to C=S and C=O carbons, respectively.

X-ray crystallography

The molecular structures of **1**–**3** have been established by single crystal X-ray crystallography, Fig. 1. All three compounds present multiple molecules in their respective crystallographic asymmetric units, i.e. four in **1** (molecules 'a', 'b', 'c', and 'd') and two in each of **2** and **3** (molecules 'a' and b'). Selected geometric parameters for **1**-**3** are collected in Table 2. The thione residue in **1** is flanked on either side by diphenyl amine and amide groups. The C1–N1 bond lengths are systematically longer than the C1–N2 bonds, Table 1. There are also systematic trends in the bond angles subtended at the C1 atom that are related to steric effects. Thus, while the S1–C1–N1 angle is close to 120º, the S1–C1–N2 angle is significantly wider, by about 5º, to relieve steric stress between the doubly bonded sulfur atom and disubstituted amine group, and this is compensated by a smaller angle subtended by the N1 and N2 atoms, Table 2. A similar situation pertains to the angles about the C2 atom with the O1–C1–N1 angles being 8-9º wider than the N1–C2–C3 angles, Table 1. The C1–N1–C2–O1 residues are co-planar with the maximum deviation, i.e. 5.9(5)º, noted for molecule 'd'. However, twists of up to 60º are

noted about the C1–N1 bond as manifested in the S1–C1–N1–C2 and N2–C1–N1–C2 torsion angles, and twists in the range 30-40º are seen about the C2–C3 bonds.

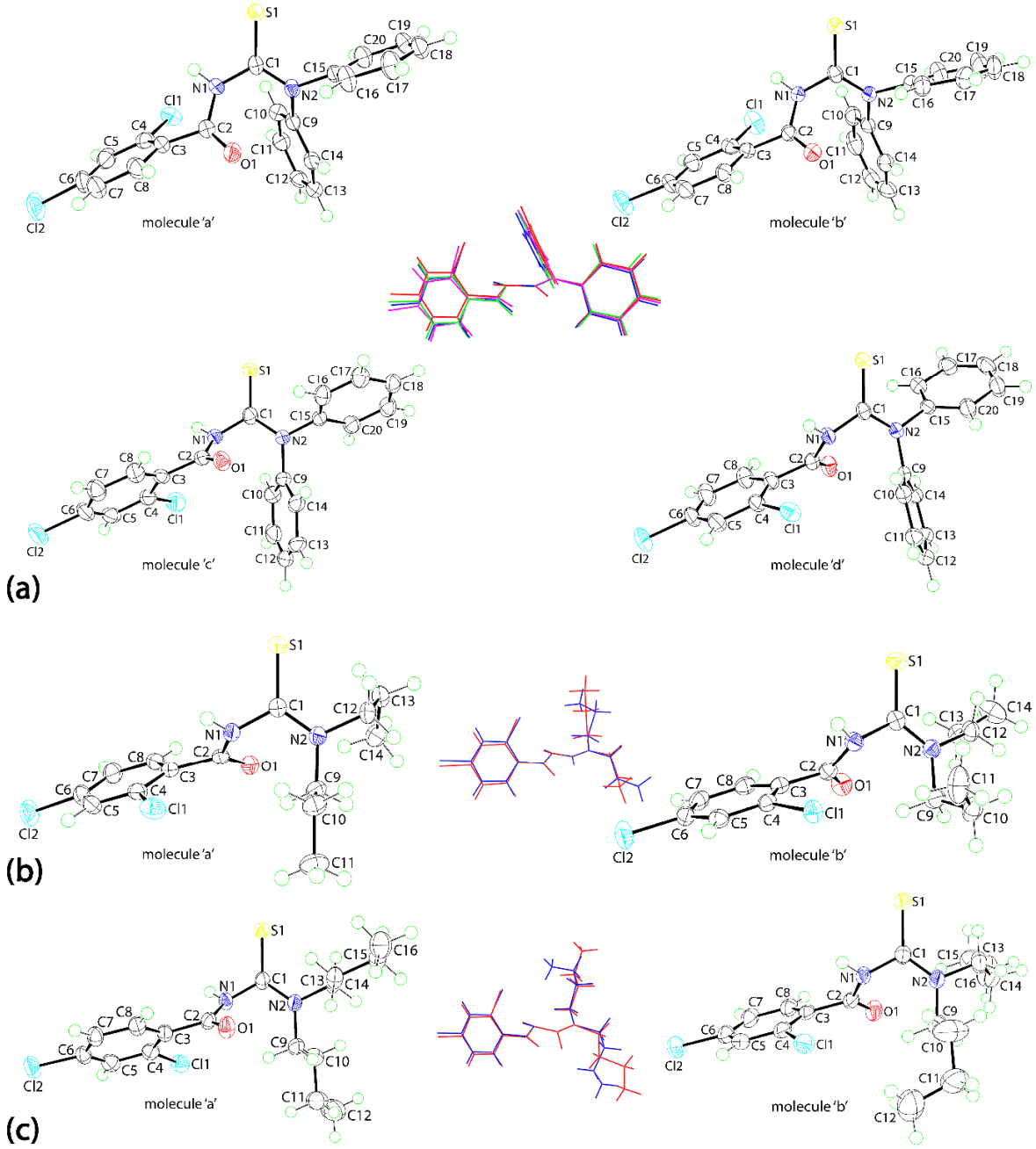

Fig. 1. (a) Molecular structures of the four independent molecules comprising the asymmetric unit of **1**, and overlay diagram showing molecules a (red image), b (green), c (blue) and inverted

d (pink), (b) the two independent molecules of **2** and overlay diagrams of molecules a (red image) and b (blue), and (c) the two independent molecules of **3** and overlay diagrams of molecules a (red image) and inverted b (blue). Only the major component of the disorder is shown in each case. For the overlay diagrams, the molecules have been overlapped so the N_2S atoms are coincident.

The same trends are noted in the C1–N1 vs C1–N2 bond lengths in **2** as for **1** (and **3**). Twists of up 12º are noted about the C1–N2 bond, Table 2, and greater twists are noted in the S1–C1–N1–C2 torsion angles, i.e. 65º. While the N1–C2–C3–C4 torsion angle in **2** are about the same as the equivalent angles in **1**, greater twists, again ca. 65º, are noted in the N2–C1–N1–C2 torsion angles. The substitution of n-propyl groups in **2** for n-butyl in **3** does not have a chemically significant impact upon the molecular geometries, with differences in torsion angles being less than 2º.

Geometric parameters characterizing the molecular packing in **1**–**3** are summarized in Table 3. The most prominent feature of the molecular packing of **1** is the formation of amine-N-H…S(thione) hydrogen bonds between molecules of 'a' and 'd', Fig. 2a, between centrosymmetrically related molecules of 'b', and between centrosymmetrically related molecules of 'c', giving rise to three distinct eight-membered $\{\ldots HNCS\}_2$ synthons. These are connected into supramolecular layers by C–H…Cl, C–H…O, involving all four independent carbonyl-O atoms, and C–H…S interactions. Layers stack along the c-axis enabling inter-digitation of the chlorophenyl rings. Layers are connected by C–Cl…π(phenyl) and C–S…π(chlorophenyl) interactions to consolidate the three-dimensional crystal, Fig. 2b.

Table 2

Selected geometric data (Å, º) for **1**–**3**.

	1a	**1**b	**1**c	**1**d	**2**a	**2**b	**3**a	**3**b
C1–S1	1.667(3)	1.656(3)	1.655(3)	1.662(3)	1.6773(13)	1.6752(13)	1.6812(17)	1.6821(18)
C1–N1	1.393(3)	1.403(3)	1.409(4)	1.404(3)	1.4251(16)	1.4168(16)	1.417(2)	1.419(2)
C1–N2	1.351(4)	1.341(4)	1.354(4)	1.347(4)	1.3242(16)	1.3290(17)	1.325(2)	1.327(2)
C2–O1	1.213(4)	1.218(4)	1.212(4)	1.219(4)	1.2279(16)	1.2204(16)	1.220(2)	1.221(2)
S1–C1–N1	120.0(2)	120.4(2)	120.2(2)	120.0(2)	117.99(9)	117.62(9)	118.29(12)	117.63(12)
S1–C1–N2	123.9(2)	124.6(2)	125.2(2)	123.8(2)	125.47(10)	125.55(10)	125.21(13)	126.22(14)
N1–C1–N2	116.1(3)	115.0(3)	114.6(3)	116.2(2)	116.53(11)	116.83(11)	116.48(15)	116.15(15)
O1–C2–N1	123.7(3)	122.6(3)	123.2(3)	123.0(3)	122.95(11)	123.32(12)	122.95(16)	123.47(16)
O1–C2–C3	121.0(3)	121.3(3)	120.5(3)	120.4(3)	119.84(11)	120.59(12)	120.18(15)	120.39(16)
N1–C2–C3	115.2(2)	116.0(3)	116.2(3)	116.5(2)	117.16(11)	116.08(11)	116.84(14)	116.11(15)
S1–C1–N1–C2	-133.6(3)	-121.3(3)	-125.2(3)	131.5(3)	114.66(11)	115.27(12)	-110.73(16)	112.65(16)
C1–N1–C2–O1	-3.0(5)	0.0(4)	-2.4(5)	5.9(5)	11.54(18)	8.68(19)	-12.9(3)	12.3(3)
N1–C2–C3–C4	49.0(4)	40.3(4)	47.1(4)	-49.5(4)	-46.72(17)	-46.54(17)	46.5(2)	-49.6(2)
N2–C1–N1–C2	48.0(4)	60.9(4)	56.5(4)	-49.0(4)	-65.86(15)	-65.25(16)	68.0(2)	-67.0(2)

Table 3

Summary of intermolecular interactions (Å, º) in **1**–**3**.

	A	H	D	H…D	A…D	A-H…D	Symmetry operation
1							
	N1a	H1a	S1d	2.47(2)	3.331(2)	168(3)	-1+x, y, z
	N1b	H1b	S1b	2.48(3)	3.323(2)	160(2)	-x, 1-y, 1-z
	N1c	H1c	S1c	2.59(3)	3.384(3)	151(3)	1-x, 1-y, -z
	N1d	H1d	S1a	2.52(2)	3.399(2)	173(3)	1+x, y, z
	C8b	H8b	Cl1c	2.79	3.734(3)	172	x, 1½-y, ½+z
	C8c	H8c	Cl1b	2.69	3.565(3)	153	x, ½-y, -½+z
	C11b	H11b	O1c	2.58	3.406(5)	146	x, ½-y, ½+z
	C13a	H13a	O1d	2.51	3.272(3)	137	x, y, z
	C13b	H13b	O1b	2.30	3.159(4)	150	1-x, 1-y, 1-z
	C13c	H13c	O1c	2.58	3.265(4)	130	-x, 1-y, -z
	C13d	H13d	O1a	2.56	3.361(4)	142	x, y, z
	C19a	H19a	S1b	2.84	3.778(4)	171	-x, -½+y, ½-z
	C6b	Cl2b	Cg(C9a-C14a)	3.5380(14)	5.082(3)	147.13(10)	x, ½-y, ½+z
	C1b	S1b	Cg(C3b-C8b)	3.6972(13)	5.235(3)	153.83(11)	-x, 1-y, 1-z
	C1c	S1c	Cg(C3c-C8c)	3.6912(14)	5.262(3)	158.08(11)	1-x, 1-y, -z

2							
	N1a	H1a	S1a	2.652(15)	3.5121(11)	170.2(13)	1-x, 1-y, 2-z
	N1b	H1b	O1a	2.156(15)	3.0216(14)	176.3(13)	x, y, z
	C10b	H10c	Cl1a	2.68	3.5893(15)	152	x, y, -1+z
	C5b	H5b	Cg(C3a-C8a)	2.76	3.4466(13)	129	1-x, 1-y, 1-z
3							
	N1a	H1a	S1b	2.576(10)	3.4542(15)	176(2)	x, -1+y, z
	N1b	H1b	S1a	2.534(11)	3.3939(15)	168(2)	x, 1+y, z
	C7a	H7a	S1a	2.87	3.8008(19)	168	x, 1+y, z
	C7b	H7b	S1b	2.77	3.709(2)	170	x, -1+y, z
	C13a	H13b	O1a	2.50	3.384(2)	149	½-x, -½+y, ½-z

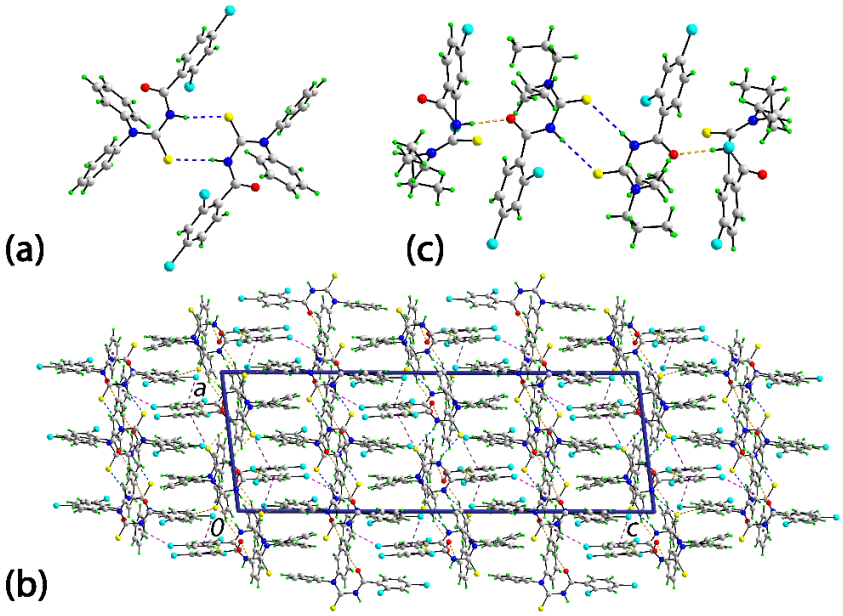
(a)
(c)
(b)
a
0
c

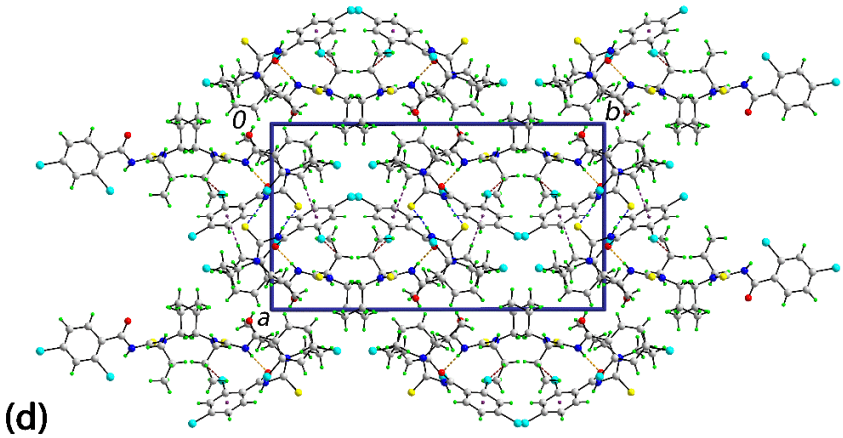
(d)
0
b
a

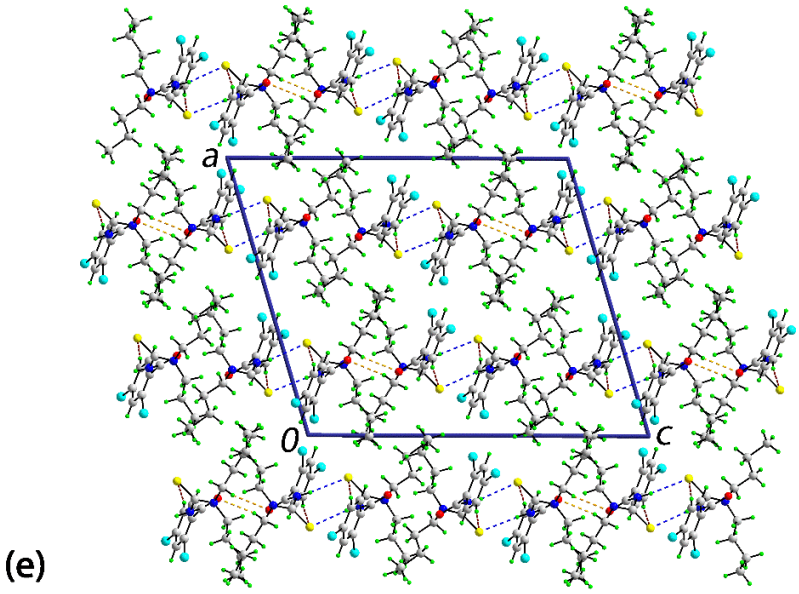
(e)
a
0
c

Fig. 2. (a) Two molecule aggregate sustained by an eight-membered {…HNCS}$_2$ synthon in **1**, (b) view in projection down the b-axis of the unit cell contents for **1**, (c) four-molecule aggregate in **2** mediated by the {…HNCS}$_2$ synthon and amide-N–H…O(carbonyl) hydrogen bonds, (d) view in projection down the c-axis of the unit cell contents for **2**, and (e) view in projection down the b-axis of the unit cell contents for **3**. The N–H…S hydrogen bonds are shown as blue dashed lines. In (b), the C–H…Cl, O and S interactions are shown as orange dashed lines while the C–Cl…π(phenyl) and C–S…π(chlorophenyl) interactions are shown as pink and purple dashed lines, respectively. In (d) the N–H…O hydrogen bonds and C–H…Cl and C–H…π interactions are shown as orange, brown and purple dashed lines, respectively. In (e) the C–H…O and C–H…S interactions are shown as orange and brown dashed lines, respectively. In (d) and (e) the inter-layer Cl…Cl halogen bonding (see text) is not shown.

In the crystal of **2**, amine-N–H…S(thione) hydrogen bonding between centrosymmetrically related molecules of 'a' leads to the formation eight-membered {…HNCS}$_2$ synthons, as for **1**. The second independent molecule associates with the dimer via amide-N–H…O(carbonyl) hydrogen bonding leading to a four molecule aggregate, Fig. 2c, Table 3. These are connected into slabs that stack along the b-axis via C–H…Cl and C–H…π(chlorophenyl) interactions. The most significant inter-layer interactions appear to be halogen bonding. While the Cl2a…Cl2b^{i} separations of 3.5686(6) Å are greater than the sum of the van der Waals radii, i.e. 3.50 Å, the crystal contains chloride-rich channels so that the interactions reinforce each other, Fig. 2d; symmetry operation i: 1-x, 1-y, 1-z.

In **3**, the two independent molecules associate via {…HNCS}$_2$ synthons, to form two-molecule aggregates, Table 3. These are connected into supramolecular layers via a combination of C–H…S and C–H…O interactions, Fig. 2e. Connections between layers along the a-axis are again halogen bonding, i.e. Cl1a…Cl1a^{i} = 3.2450(7) Å; symmetry operation i: 1-x, -y, 1-z.

Antioxidant activity

Reactive oxygen species (ROS) are produced in the body as a result of incomplete reduction of oxygen during oxidative phosphorylation [34]. Free radicals can attack DNA and results in mutation and cancer [35]. Free radicals can also react with proteins, carbohydrates and lipids and plays a significant role in the pathogenesis of numerous disorders and patho-physiological processes including cardiovascular diseases, diabetes, and cancer [36]. Oxidative stress occurs, when the system loses its ability to neutralize the excessively produced reactive species. The redox homeostasis, i.e. the balance between the free radicals and antioxidants is necessary for maintaining good health. This balance is maintained by a number of antioxidants (vitamin E and ascorbic acid) and enzymes like catalase, glutathione peroxidise, glutathione-S-transferase, superoxide dismutase, etc. Under severe conditions, above-mentioned antioxidant system is not sufficient to prevent the oxidative stress. Hence, intake of external anti-oxidants is necessary for maintaining homeostasis in the body. In this connection, several attempts have been made to synthesize molecules and their derivatives with effective antioxidant property in the past [20,21,37,38]. In the present study also, we have evaluated the antioxidant activity of the three amine acyl thiourea derivatives, **1**–**3**, as summarized in Fig. 3.

In the phosphomolybdate assay, molybdenum(VI) is reduced to molybdenum(V) by an antioxidant to forms a green complex at acidic pH in the presence of phosphorous with an

absorption maxima at 695 nm. This assay evaluates the reducing or electron donating power of the antioxidant to molybdenum with the intensity of phosphomolybdate (PMo(V)) complex being proportional to antioxidant power of the extract. The reducing capacity of the trial compound may serve as a significant indicator of its potential antioxidant ability. Among the presently analyzed compounds, **2** recorded a higher level of phosphomolybdate reducing power in dose-dependent manner, Fig. 3a. In the ferric reducing assay, iron(III) is reduced to iron(II) by the antioxidant compound through electron transfer. The reduced iron(II) forms the Pearl's blue complex, which can be measured at 700 nm. Fig. 3b reveals the ferric reducing power of presently investigated compounds and that **2** registered the maximum ferric reducing activity when compared to the other two compounds.

DPPH (2,2-Diphenyl-1-picrylhydrazyl) is a stable radical, the methanolic solution of which is dark-purple with a maximum absorption at 515 nm. The evaluation of the antioxidant power by DPPH radical scavenging activity has been widely used for different plant extracts and synthetic compounds. Antioxidants can reduce DPPH through hydrogen transfer into its non-radical form (DPPH-H) and hence the absorption disappears at 515 nm. The decrease in absorbency at 515 nm may be due to the reaction between phytochemicals and DPPH, which indicates the antioxidant power. In the present study, **2** recorded the highest DPPH radical scavenging activity, which is followed by **3** and **1**, Fig. 3c.

Superoxide radical is an oxygen molecule with one unpaired electron. Superoxide is biologically quite toxic and is deployed by the immune system to kill invading microorganisms. In phagocytes, superoxide is produced in large quantities by the enzyme NADPH oxidase for use in oxygen-dependent killing mechanisms of invading pathogens. Although the superoxide anion is a weak oxidant, it gives rise to the generation of powerful and dangerous hydroxyl radicals as

well as singlet oxygen, both of which contribute to the oxidative stress. The superoxide radical scavenging activity of samples was investigated by generating superoxide through photo-induced reduction of riboflavin, which can generate superoxide radical in the presence of methionine. The generated superoxide radical reduce the NBT into purple formazan, which was evaluated at 560 nm. In presence of antioxidant, the generated superoxide radicals were scavenged and hence, formation of purple formazan is minimal or nil. The superoxide radical scavenging activity of the synthesized compounds is represented in Fig. 3d with …give summary of the key result(s)…

Anticancer activity

Cancer is often associated with increased risk of death and the toxic side effects caused by the modern medicine, many cancer patients seek alternative and complementary methods of treatment such as usage of phytomedicine [39]. At present chemotherapy is considered as the most efficient approach for cancer treatment. Even though it significantly improves symptoms and the quality of life of cancer patients, only modest increases in survival rate can be achieved. As a palliative care, many cancer patients use herbal therapies. Medicinal plants are well known for their free radical scavenging and antioxidant activities [40]. Free radical attack results in the oxidative damage of various biomolecules including lipids, proteins and DNA. The damage caused in DNA leads to mutation or cancer, which is the most dangerous effect in human beings. Plants contain phytochemicals with strong antioxidant activities which may prevent and control cancer and other diseases by protecting the cells from the deleterious effects of the free radicals. In the present time researchers are focusing their research towards the development of eco-friendly anticancer drugs, which resulted in the development of novel chemotherapeutic agents such as paclitaxel, vincristine, podophyllotoxin, and camptothecin.

The newly synthesized acylthiourea derivatives **1**–**3** were screened for anticancer potential against Ehrlich Ascites Carcinoma (EAC) cell lines employing the MTT assay with a view to develop a natural and safe anticancer drug. Among the compounds tested, **2** revealed remarkable level of anticancer effect, Fig. 4. Cytotoxicity was found to be at a maximum even at very low concentrations, and the death of the cells caused by the test compound might be due to the loss of mitochondria [41]. From the MTT assay, it is evident that the cytotoxicity of the extracts against EAC cell line was dose dependent.

Similar to the present study, Hallur et al. reported the anticancer activity of benzoylphenylurea sulfur analogues in breast, pancreatic and propstate cancer cell lines [20]. Saeed et al. also evaluated the anticancer activity of some thiourea derivatives bearing benzothiazole moiety in MCF-7 and Hela cell lines [21]. Further, the cytotoxic effect of nickel(II) complexes synthesized using the 3,3-dialkyl/aryl-1-(2,4-dichlorobenzoyl) thiourea ligands has been investigated in human lung cancer (A549) and colon cancer cell lines (HT29) [37]. Based on the results obtained from the present study, **2** was found to be more effective in controlling the growth of EAC cell lines when compared to other extracts. Hence, it could be considered as a source of potential anticancer drug and further *in vivo* models must be used to explore the potential of this compound for clinical use.

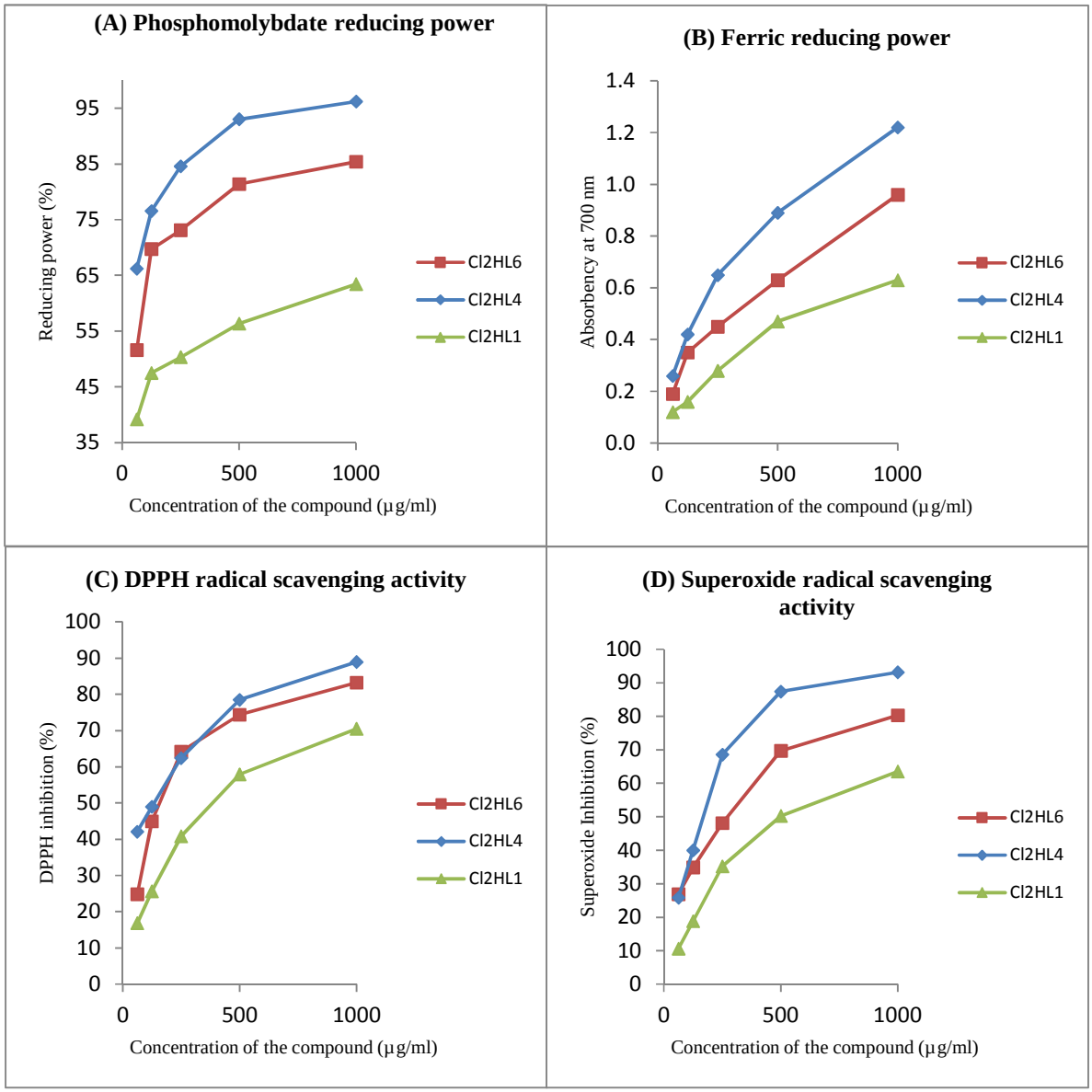

Fig. 3. Antioxidant activity of synthesized compounds: (a) phosphomolybdate reducing power, (b) Ferric reducing power, (c) DPPH radical scavenging activity, and (d) superoxide radical scavenging activity.

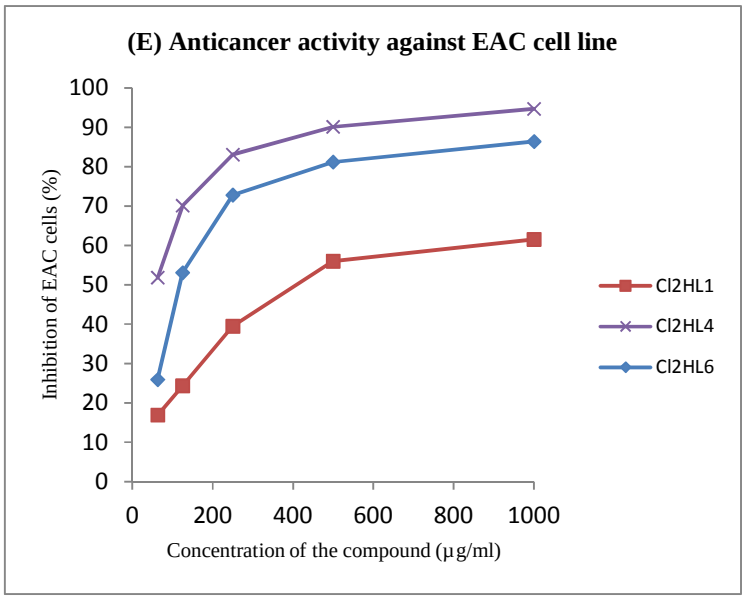

Fig. 4. Anticancer activity of **1**–**3** against the EAC cancer cell line.

Conclusions

In summary, three acylthiourea derivatives, **1**–**3**, were prepared and characterized by analytical and spectral methods. Three dimensional structures of all three compounds were derived by single crystal X-ray crystallography. The acylthiourea derivatives were subjected to *in vitro* antioxidant and anticancer studies. The results indicated that **2** is more effective in exhibiting antioxidant and anti-cancer properties when compared to other compounds. This might be due to the steric effect of the molecule through which it could activate the functional groups and exhibited the remarkable antioxidant and anticancer potentials. On the other hand, the low levels of antioxidant and anticancer activities of other two compounds (**1** and **3**) might be due to the hindrance effects, which might down-regulate the effect of functional groups. Hence,

based on the preliminary study, the **2** was selected for further study as it shows promising antioxidant and anticancer activities. Further details research is necessary to investigate the anticancer potential of this compound in suitable animal model and also to reveal the mechanism of action / pathway through which **2** induces apoptosis and effectively arrest the cell proliferation.

Acknowledgements

N.G. gratefully acknowledges DST, Government of India, for financial assistance under SERB Start-Up Research Grant scheme for Young Scientists (No.SB/FT/CS-189/2013) and SASTRA University for Prof. TRR fund and the infrastructural support.

Appendix A. Supplementary material

CCDC 493453-1493455 contain the supplementary crystallographic data for this paper. These data can be obtained free of charge from The Cambridge Crystallographic Data Centre via www.ccdc.cam.ac.uk/data_request/cif. Supplementary data associated with this article can be found, in the online version.

References

[1] K.R. Koch, Coord. Chem. Rev. 216 (2001) 473–488.

[2] M.M. Habtu, S.A. Bourne, K.R. Koch, R.C. Luckay, New J. Chem. 30 (2006) 1155–1162.

[3] N. Gunasekaran, N. Remya, S. Radhakrishnan, R. Karvembu, J. Coord. Chem. 64 (2011) 491–501.

[4] N. Gunasekaran, R. Karvembu, Inorg. Chem. Commun. 13 (2010) 952–955.

[5] N. Gunasekaran, P. Ramesh, M.N. Ponnusamy, R. Karvembu, Dalton Trans. 40 (2011) 12519–12526.

[6] N. Gunasekaran, P. Jerome, S.W. Ng, E.R.T. Tiekink, R. Karvembu, J. Mol. Catal. A: Chem. 353–354 (2012) 156–162.

[7] K. Chandrasekhara, R. Pillai, J. Narayan, J. Electrochem. Soc. 125 (1978) 1393–1397.

[8] M. Ozcan, I. Dehri, M. Erbil, Appl. Surf. Sci. 236 (2004) 155–164.

[9] S.S. Abdel-Rehim, K.F. Khaled, N.S. Abd-Elshafi, Electrochim. Acta. 51 (2006) 3269–3297.

[10] R.-S. Zeng, J.-P. Zou, S.-J. Zhi, J. Chen, Q. Shen, Org. Lett. 5 (2003) 1657–1659.

[11] G.N. Lipunova, E.V. Nosova, A.A. Laeva, T.V. Trashakhova, P.A. Slepukhin, V.N. Charushin, Russ. J. Org. Chem. 44 (2008) 741−749.

[12] Z. Zhong, R. Xing, S. Liu, L. Wang, S. Cai, P. Li, Carbohydr. Res. 343 (2008) 566–570.

[13] A. Saeed, U. Shaheen, A. Hameed, S.Z.H. Naqvi, J. Fluorine Chem. 130 (2009) 1028–1034.

[14] M. Eweis, S.S. Elkholy, M.Z. Elsabee, Int. J. Biol. Macromol. 38 (2006) 1–8.

[15] K. Ramadus, G. Suresh, N. Janarthanan, S. Masilamani, Pestic. Sci. 52 (1998) 145–151.

[16] X. Xu, X. Qian, Z. Li, Q. Huang, G. Chen, J. Fluorine Chem. 121 (2003) 51–54.

[17] X. Sijia, D. Liping, K. Shaoyong, J. Liangbin, Chem. J. Internet 5 (2003) 67–70.

[18] C. Sun, H. Huang, M. Feng, X. Shi, X. Zhang, P. Zhou, Bioorg. Med. Chem. Lett. 16 (2006) 162–166.

[19] W. Hermindez, E. Spodine, L. Beyer, U. Schrtider, R. Richter, J. Ferreira, M. Pavani, Bioinorg. Chem. Appl. 3 (2005) 299–316.

[20] G. Hallur, A. Jimeno, S. Dalrymple, T. Zhu, M.K. Jung, M. Hidalgo, J.T. Isaacs, S. Sukumar, E. Hamel, S.R. Khan, J. Med. Chem. 49 (2006) 2357–2360.

[21] S. Saeed, N. Rashid, P.G. Jones, M. Ali, R. Hussain, Eur. J. Med. Chem. 45 (2010) 1323–1331.

[22] Agilent Technologies, CrysAlis PRO. Yarnton, Oxfordshire, England, 2015.

[23] G.M. Sheldrick, Acta Cryst. A64 (2008) 112–122.

[24] L.J. Farrugia, J. Appl. Crystallogr. 45 (2012) 849–854.

[25] G.M. Sheldrick, Acta Cryst. C71 (2015) 3–8.

[26] J. Gans, D. Shalloway, J. Mol. Graph. Model. 19 (2001) 557–559.

[27] K. Brandenburg, DIAMOND, Crystal Impact GbR, Bonn, Germany, 2006.

[28] A.L. Spek, J. Appl. Crystallogr. 36 (2003) 7–13.

[29] P. Prieto, M. Pineda, M. Aguilar, Anal. Biochem. 269 (1999) 337–341.

[30] M. Oyaizu, Jpn. J. Nutr. 44 (1986) 307–315.

[31] C. Sanchez-Moreno, J.A. Larrauri, F.A. Saura-Calixto, J. Sci. Food Agr. 76 (1998) 270–276.

[32] J. Zhishen, T. Mengcheng, W. Jianming, Food Chem. 64 (1999) 555–559.

[33] T. Mosmann, J. Immunol. Methods 65 (1983) 55–63.

[34] C. Nathan, J. Clin. Invest. 111 (2003) 769–778.

[35] M. Perse, Bio. Med. Res. Int. (2013) Article ID 725710.

[36] A. Federico, F. Morgillo, C. Tuccillo, F. Ciardiello, C. Loguercio, Int. J. Cancer 121 (2007) 2381–2386.

[37] N. Selvakumaran, N.S.P. Bhuvanesh, A. Endo, R. Karvembu, Polyhedron 75 (2014) 95–109.

[38] J. Haribabu, G.R. Subhashree, S. Saranya, K. Gomathi, R. Karvembu, D. Gayathri, J. Mol. Struct. 1094 (2015) 281–291.

[39] J. Kim, E.J. Park, Cur. Med. Chem. Anticancer Agent 20 (2002) 485–537.

[40] S.K. Agarwal, S. Chatterjee, S.K. Misra, Phytomedica 2 (2001) 1–22.

[41] S.P. Christopher, Cancer Metstat. Rev. 11(1992) 179–195.